

Low-Velocity Impact Response of Smart Sandwich Composite Plates with Piezoelectric Transducers: Modeling and Experiment

Theofanis S. Plagianakos^{1*}, Klajd Lika² and Evangelos G. Papadopoulos³

¹ Post-Doctoral Fellow, Department of Mechanical Engineering, National Technical University of Athens, Greece

² Research Assistant

³ Full Professor

Abstract

A global-local methodology is presented for predicting the response of sandwich composite plates with piezoelectric transducers to low-velocity impact. Model reduction techniques have been employed in order to build a computationally efficient plate-impactor structural system, solution of which yields the global plate's response. Higher-order layerwise kinematic assumptions enable estimation of the stress distribution locally through the thickness of the laminate and prediction of stress at the interface between different materials. Using the developed method, impact identification studies have been conducted in order to estimate impact location and impactor mass and velocity, and to reconstruct the impact event, including impact force history, posteriori. In order to validate the developed methodology, a low-cost experimental configuration for impact-testing has been designed and impact measurements were compared to the predictions.

1. INTRODUCTION

Smart sandwich plates with composite faces, foam core and surface-attached piezoelectric transducers combine the superior mechanical properties of sandwich structures, such as, high flexural stiffness to mass ratio, with the capability to monitor the structural response on-site in real-time and to adapt their response according to selected control criteria. In this kind of structures, the high thickness and strong inhomogeneity through the thickness may lead to delamination between piezoelectric and composite material layer at high loading rates, such as in the case of impact loading, whereas in low-velocity impact this damage may be invisible. Thus, prediction of the global dynamic response and local through-thickness stress field is essential in order to keep structural design within appropriate safety limits. Moreover, monitoring of the impact response and reconstruction of the impact event by means of piezoelectric transducers could reduce the probability of this damage to remain unrevealed.

Impact on composite and sandwich structures has been a hot research topic in the last three decades ([1]-[2]). Depending on the kinematic approximation used for modeling the impacted structure, the existing models for predicting its impact response may be divided to (i) mass-spring models [3] and (ii) full continuum models based on energy equilibrium equations [4]. The contact law between structure and impactor may be Hertzian, elastoplastic with/without permanent indentation [5] and take into account core crushing and damage in general [6]. Several analytical and finite element solutions for predicting impact

* Corresponding author, fanplag@gmail.com

response of composite and sandwich plates have been developed. Most of these solutions are based on single-layer through-thickness kinematic assumptions [7]-[8]. Icardi and Ferrero reported a refined plate element based on global-local 3-D layerwise kinematic assumptions and predicted distributions of transverse displacement and interlaminar shear stress across the thickness of the plate and impact-induced damage [9]. The impact response of composite plates with piezoelectric transducers has been initially studied by Chang and coworkers [10]-[11] in order to identify impact location and achieve impact force reconstruction. Later works elaborated these basic ideas towards the design of real-time monitoring networks ([12]-[16]). Saravanos and Christoforou studied the active minimization of impact force in composite shells with piezoelectric layers by means of state- and output-feedback control algorithms [17]. Yet, no integrated methodologies have been reported for predicting both global (impact force and plate deflection) and local through-thickness response of composite and sandwich composite plates with piezoelectric transducers. Moreover, the impact identification techniques proposed so far lead to impact source localization and force history reconstruction, whereas it would be also useful for both design and inspection stage to be able to estimate parameters such as impactor mass and velocity and recreate the local through-thickness response.

Towards this direction, the authors recently reported a computationally efficient methodology based on modal reduction for predicting the global and the local response in composite and sandwich composite plates with piezoelectric sensory layers [18]. In the present paper the impact response of sandwich structures impacted at random impact locations are shown and the methodology is used backwards as a posteriori impact identification tool. In addition, a low-cost impact testing configuration is described and used for conducting validation studies in isotropic sandwich plates.

2. IMPACT MECHANICS METHODOLOGY

The following paragraphs give the main idea of the global-local impact mechanics methodology, which has been developed for predicting the response of composite and sandwich composite plates with sensory and/or active piezoelectric layers or patches. A more detailed description can be found in [18].

2.1 Basic Physical Assumptions

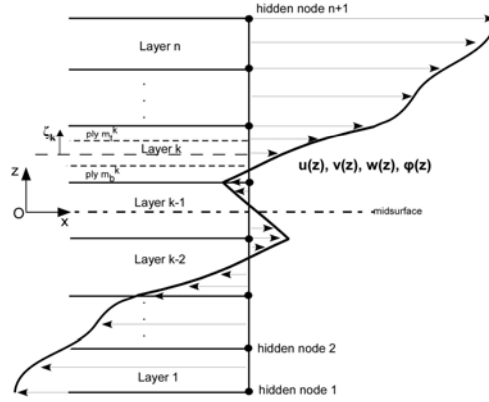
The following physical assumptions have been made for the impact event, the impacting bodies and their interaction:

- The impact energy is low, such as no material damage is induced.
- The impact is elastic, thus there is no energy loss in the form of heat.
- The laminate plies are perfectly bonded together throughout the impact and subsequent vibration.

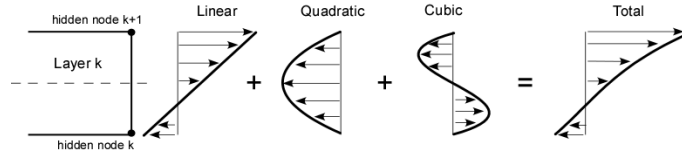
Generally, impacts may be categorized to low- and high-velocity ones on the basis of the overall structural response [2]. In the present formulation it is assumed that the impact duration is significantly longer than the travel time of the waves to the boundary, and is enough for the plate to respond [1]. The impact velocities studied are up to 3 m/s.

2.2 Through-Thickness Plate Kinematics

A typical composite or sandwich composite laminate with piezoelectric transducers is subdivided into n discrete layers as shown schematically in Figure 1.



(a)



(b)

Figure 1: Typical sandwich piezoelectric composite laminate configuration analyzed with n -discrete layers. (a) Discrete layers. (b) Assumed displacement and electric potential distribution in each layer.

The through-thickness distribution of displacements and electric potential is approximated by superposition of piecewise linear, quadratic and cubic polynomial functions. The contributions of the higher-order variations vanish at the interfaces between discrete layers and at free faces, so as to ensure continuity a priori. In this context the through-thickness displacement and electric potential fields take the form:

$$\begin{aligned}
 \mathbf{u}^k(x, y, \zeta_k) &= U^k(x, y)\Psi_1^k(\zeta_k) + U^{k+1}(x, y)\Psi_2^k(\zeta_k) + \alpha_x^k(x, y)\Psi_3^k(\zeta_k) + \lambda_x^k(x, y)\Psi_4^k(\zeta_k) \\
 \mathbf{v}^k(x, y, \zeta_k) &= V^k(x, y)\Psi_1^k(\zeta_k) + V^{k+1}(x, y)\Psi_2^k(\zeta_k) + \alpha_y^k(x, y)\Psi_3^k(\zeta_k) + \lambda_y^k(x, y)\Psi_4^k(\zeta_k) \\
 \mathbf{w}^k(x, y, \zeta_k) &= W^k(x, y)\Psi_1^k(\zeta_k) + W^{k+1}(x, y)\Psi_2^k(\zeta_k) + \alpha_z^k(x, y)\Psi_3^k(\zeta_k) + \lambda_z^k(x, y)\Psi_4^k(\zeta_k) \\
 \Phi_z(x, y, \zeta_k) &= \Phi_z^k(x, y)\Psi_1^k(\zeta_k) + \Phi_z^{k+1}(x, y)\Psi_2^k(\zeta_k) + \alpha_\phi^k(x, y)\Psi_3^k(\zeta_k) + \lambda_\phi^k(x, y)\Psi_4^k(\zeta_k)
 \end{aligned} \tag{1}$$

where \mathbf{u} and \mathbf{v} are the in-plane displacements, \mathbf{w} is the transverse displacement, superscripts $k=1, \dots, n$ denote discrete layer and ζ_k is the local thickness coordinate of layer k defined such that $\zeta_k=0$ at the middle of the discrete layer, $\zeta_k=1$ and $\zeta_k=-1$ at the top and the bottom, of the discrete layer k , respectively. Ψ_1^k, Ψ_2^k are linear and Ψ_3^k, Ψ_4^k are quadratic, cubic interpolation functions, respectively, through the thickness of the layer. $U^k, V^k, W^k, U^{k+1}, V^{k+1}, W^{k+1}$ and Φ_z^k, Φ_z^{k+1} are displacements and electric potential at the bottom and top of the discrete layer k , effectively describing extension and rotation, and electric potential at the terminals, respectively, of the layer. By assuming constant through-thickness transverse displacement the above kinematic assumptions become computationally efficient in predicting the response of monolithic isotropic or composite plates.

It should be noted that the approximations of eq. (1) yield up to cubic order layerwise distributions of in-plane normal, shear and interlaminar shear strains, whereas piecewise quadratic distributions of transverse normal strain can be predicted [19]. The through-thickness shear stress continuity is weakly maintained through the equations of electromechanical equilibrium in order to keep the formulation simple and to preserve C^0 continuity. In the case of constant through-thickness deflection interlaminar

shear stress continuity is explicitly imposed, leading to C^1 continuous in-plane approximations of transverse displacement.

2.3 In-Plane Approximation of Elastic-Electric Variables

In the case of a Ritz-type analytical solution, the first order electromechanical variables are approximated by Fourier series expansions, which are expressed in a general form as,

$$\begin{aligned} W^k(x, y) &= \sum_i^m \sum_j^n \bar{W}_{ij}^k X_{ij}^w(x, y) & V^k(x, y) &= \sum_i^m \sum_j^n \bar{V}_{ij}^k X_{ij}^v(x, y) \\ U^k(x, y) &= \sum_i^m \sum_j^n \bar{U}_{ij}^k X_{ij}^u(x, y) & \Phi^k(x, y) &= \sum_i^m \sum_j^n \bar{\Phi}_{ij}^k X_{ij}^\phi(x, y) \end{aligned} \quad (2)$$

where m, n denote modes along x and y , respectively, and X_{ij} are approximation functions of each variable indicated by superscript, which are derived by satisfying the arbitrary boundary conditions [20]. The higher-order terms of displacement and electric potential are approximated accordingly on the basis of the first-order variable they refer to. The impact load is assumed to act transversely at the impact point and is approximated using the approximation functions of the transverse displacement. The general form of the above approximations includes Navier-type solutions applicable for cross-ply simply-supported plates.

2.4 Plate Modal Matrices and Implementation of Reduction Techniques

The plate structural subsystem in discrete form for each vibration mode pair mn is built by combining the equations of motion with the strain-displacement relations, constitutive equations and in-plane approximations (2):

$$\begin{bmatrix} [M_{uu}]_{mn} & 0 \\ 0 & 0 \end{bmatrix} \begin{Bmatrix} \bar{\mathbf{u}}_{mn} \\ \bar{\boldsymbol{\phi}}_{mn}^{-P} \end{Bmatrix} + \begin{bmatrix} [K_{uu}]_{mn} & [K_{u\phi}^{PP}]_{mn} \\ [K_{\phi u}^{PP}]_{mn} & [K_{\phi\phi}^{PP}]_{mn} \end{bmatrix} \begin{Bmatrix} \bar{\mathbf{u}}_{mn} \\ \bar{\boldsymbol{\phi}}_{mn}^{-P} \end{Bmatrix} = \begin{Bmatrix} \mathbf{q}_{mn}(t) - [K_{u\phi}^{PA}]_{mn} \bar{\boldsymbol{\phi}}_{mn}^{-A} \\ \mathbf{D}_{mn}^P(t) - [K_{\phi\phi}^{PA}]_{mn} \bar{\boldsymbol{\phi}}_{mn}^{-A} \end{Bmatrix} \quad (3)$$

where superscripts P and A denote passive (sensory) and active piezoelectric layers, and

$$\begin{aligned} \bar{\mathbf{u}}_{mn} &= \left\{ W_{mn}^k, U_{mn}^k, V_{mn}^k, \alpha_{z_{mn}}^l, \alpha_{x_{mn}}^l, \alpha_{y_{mn}}^l, \lambda_{z_{mn}}^l, \lambda_{x_{mn}}^l, \lambda_{y_{mn}}^l \right\}^T \\ \bar{\boldsymbol{\phi}}_{mn}^{-P} &= \left(\left\{ \Phi_{z_{mn}}^k, \alpha_{\phi_{mn}}^l, \lambda_{\phi_{mn}}^l \right\}^P \right)^T \end{aligned} \quad (4)$$

with $k=1, \dots, n$ and $l=1, \dots, n-1$ are the plate modal elastic and electric variable vectors. The vector \mathbf{q} contains the externally applied loads per unit area, while \mathbf{D} is the vector of externally applied charges. In the absence of external charge sources, the structural subsystem is condensed as [17],

$$[M_{uu}]_{mn} \bar{\mathbf{u}}_{mn} + [K_{cu}]_{mn} \bar{\mathbf{u}}_{mn} = \mathbf{q}_{mn}(t) + [K_{ce}^A]_{mn} \bar{\boldsymbol{\phi}}_{mn}^{-A} \quad (5)$$

where

$$[K_{cu}]_{mn} = [K_{uu}]_{mn} - [K_{u\phi}^{PP}]_{mn} [K_{\phi\phi}^{PP}]_{mn}^{-1} [K_{\phi u}^{PP}]_{mn}^T \quad (6)$$

$$[K_{ce}^A]_{mn} = [K_{u\phi}^{PP}]_{mn} [K_{\phi\phi}^{PP}]_{mn}^{-1} [K_{\phi\phi}^{PA}]_{mn} - [K_{u\phi}^{PA}]_{mn} \quad (7)$$

As indicated by equations (4) and (5), the size of the mass and stiffness matrices of the plate depend on the through-thickness discretization. For a plate discretized through-thickness by n discrete layers,

equation (4) yields $9n+3$ independent elastic variables ($4n+1$ in the case of constant through-thickness deflection). These elastic variables determine the size of the mass and stiffness matrix in equation (5). Considering that for predicting the dynamic response of a plate subjected to a point impact the plate-impactor system should be solved for a large amount of mode pairs at each time step, the layerwise through-thickness discretization would lead to mass and stiffness matrices of large size and respective computational cost. In order to reduce this cost and enable implementation of the methodology to real-time control applications, while retaining the information regarding the through-thickness response, two types of reduction have been implemented: (i) A Guyan reduction scheme in the case of Ritz-type Navier solutions [19] and (ii) reduction by means of the modal vectors in the case of other boundary conditions and finite element approximations. The idea behind both reduction techniques is to select a primary (independent) elastic variable and express it as a function of the reduced (dependent) ones. Since the impact force is assumed to act purely in the z -direction (Figure 2) and thus bending vibration modes are primarily excited, the transverse displacements of bottom and top face were selected as the independent variables in both reduction schemes. In the case of the Guyan reduction, the modal vector is related to the transverse displacements as,

$$\bar{\mathbf{u}}_{mn} = \begin{Bmatrix} \mathbf{W}_{mn}^k \\ \mathbf{U}_{mn}^k \\ \mathbf{V}_{mn}^k \\ \alpha_{x_{mn}}^l \\ \alpha_{y_{mn}}^l \end{Bmatrix} = \begin{Bmatrix} -i \\ \mathbf{u}_{mn} \\ -d \\ \mathbf{u}_{mn} \end{Bmatrix} = \mathbf{T}_{mn} \bar{\mathbf{u}}_{mn} = \mathbf{T}_{mn} \begin{Bmatrix} \mathbf{W}_{mn}^l \\ \mathbf{W}_{mn}^{n+1} \end{Bmatrix} \quad (8)$$

where $k=1, \dots, n+1$, n , $l=1, \dots, n-1$ and n is the total number of discrete layers and \mathbf{T}_{mn} is the modal transformation vector. In this context, the plate stiffness matrix for each mode pair mn is reduced as:

$$\mathbf{K}_{mn}^r = \mathbf{T}_{mn}^T [\mathbf{K}_{cu}]_{mn} \mathbf{T}_{mn} \quad (9)$$

Thus the plate matrices reduction procedure yields per mode pair mn two terms for stiffness and mass, respectively (1 term in the case of constant through-thickness deflection), which increases dramatically the computational efficiency of the current methodology compared to single-layer or layerwise models, which include all terms in the structural system to be solved for each time step.

2.5 Contact Law

In the present methodology, impactors with hemi-spherical tip are considered. Linear contact laws [5] are implemented in order to retain low computational cost and facilitate implementation to real-time control applications. During impact at a point (x_0, y_0) , the contact force F_i is assumed to vary linearly with the local indentation, which is defined as the relative distance between the impactor position and the impacted face deflection:

$$F_i(x_0, y_0) = \begin{cases} k_y (w_i - W^l(x_0, y_0)) & , w_i > W^l(x_0, y_0) \\ 0 & , w_i \leq W^l(x_0, y_0) \end{cases} \quad (10)$$

where w_i is the vertical distance of the impactor (modelled as a point mass) from the plate's surface position just before impact and k_y is the contact stiffness, which depends on impactor radius and elastic properties of impactor and plate material. The above contact model is shown schematically in Figure 2 for the case of constant through-thickness deflection.

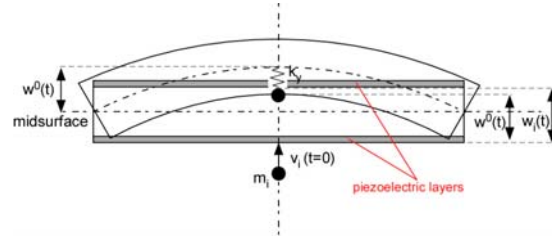


Figure 2: Linear contact model implemented during impact on a composite plate with piezoelectric layers.

2.6 Plate-Impactor Structural System

The plate-impactor structural system is formulated by combining the plate subsystem (3) with the contact force equation (10), the governing equation of motion of the impactor

$$m_i \ddot{w}_i(t) = -F_i(x_0, y_0, t) \quad (11)$$

and the expression of transverse modal load per unit area q_{mn} by means of Fourier series terms. Thus, the coupled plate-impactor system is formulated in time domain as,

$$[M_s] \begin{Bmatrix} \ddot{W}_{mn}^1(t) \\ \ddot{W}_{mn}^{n+1}(t) \\ \ddot{w}_i(t) \end{Bmatrix} + [K_s] \begin{Bmatrix} W_{mn}^1(t) \\ W_{mn}^{n+1}(t) \\ w_i(t) \end{Bmatrix} = 0 \quad (12)$$

The above system is finally transferred to state-space in order to facilitate real-time control applications:

$$\begin{aligned} \dot{\underline{x}} &= [A]\underline{x} + [B]\phi^A \\ \underline{y} &= [C]\underline{x} \end{aligned} \quad (13)$$

where $[A]$, $[B]$, $[C]$ are the system, input and output matrix, respectively and

$$\underline{x} = \{W_{mn}^1, W_{mn}^{n+1}, w_i, \dot{W}_{mn}^1, \dot{W}_{mn}^{n+1}, \dot{w}_i\}^T \quad (14)$$

is the vector of state variables. Depending on the case study, the output variables vector \underline{y} may include sensory electric potentials, mechanical displacements, strains and stresses or related time derivatives.

3. IMPACT IDENTIFICATION

Equation (13) describes the impact response of a sandwich plate impacted by a mass m_i with an initial velocity v_0 at point P with coordinates (x_p, y_p) by taking into account a contact stiffness k_y determined by involved materials and mass radius. A key prediction, which characterizes the type of impact, is the prediction of impact force (10). Inversely, if part of the output variables vector is known, for instance the signals at sensors placed at known locations on a plate's surface, an impact source identification and a reconstruction of force time history can be made by means of constrained optimization techniques [10]. The present methodology extends this idea by identifying parameters contributing to the impact force time history, namely impactor mass and initial velocity, in addition to the estimation of impact location. The identification technique may be outlined in the following steps:

- Observation of the measured sensory signals leads to estimation of the end of the impact event (t_d , d denotes disaggregation) and the quarter of the plate in which the impact occurred. A vector of measured sensory values (voltage) for each time step up to the end of impact is built.

- A scan through values of the four parameters to be identified (m_i, v_0, x_p, y_p) is conducted within a preliminary range. Using the developed methodology, sensory signals are predicted for each parameter values combination. These predictions are compared to the measured values and the following cost function is determined as a measure of the deviation:

$$J = \sum_{i=1}^N (y_m^j(i) - y_e^j(i))^2 \quad (15)$$

where subscripts m and e indicate measured and estimated values, N is the total number of time steps and $j=1, \dots, n_s$ denotes sensor. The output values of the scan are the ones that minimize the cost function and are used as first guesses for the subsequent step.

- Non-linear constrained optimization algorithms are implemented in a shorter range around the first guesses ($\pm 10\%$) to minimize the cost function, yielding the estimated values for the parameters to be identified.

Thus, in view of practical applications, the elaboration of signals provided by piezoelectric sensors placed at random known locations leads to recognition of the impact location, the mass that hit the target and its initial velocity. The proposed method has been developed for implementation in a phase of posteriori inspection of the sensory signals.

4. EXPERIMENTAL CONFIGURATION

In order to validate the predictions of the impact methodology, a low-cost portable impact testing configuration has been designed and set up (Figure 3).



Figure 3: Low-energy impact testing configuration

It consisted of a light Aluminum frame, prestressed by steel cables for providing extra rigidity, and an instrumented impactor configured to act as a pendulum, while the perpendicularity of impact was ensured by means of two parallel bearing sets. The impact force and impactor velocity were measured by a low-cost custom force sensor [21] and an encoder, respectively. The impactor was left to fall free from a predefined height. The plate specimens were mounted on the frame by screws, which were tight or loose for yielding clamped or simply-supported boundary conditions, respectively. Piezoceramic patches were attached on the back surface of the plate (opposite to the impacted face). The signals from force sensor and encoder were amplified, digitized and finally driven to a laptop for elaboration using Matlab software, whereas the signals from the piezoelectric transducers were acquired and stored using an oscilloscope. Sandwich specimens were fabricated in situ, by gluing Aluminum faces on foam core, and tested.

5. RESULTS AND DISCUSSION

Validations of the proposed method for composite and sandwich plates hit at their centre have been conducted in a preceding paper [18]. In the next paragraphs sandwich configurations with piezoelectric layers or patches are studied for the case of eccentric impact. Predictions of both global (impact force, deflection, sensory signal) and local through-thickness (displacement, stress) response are shown. Impact identification is presented for a sandwich plate with piezoceramic patches. Impact testing measurements are shown for a sandwich plate with metal faces and foam core. The electromechanical properties of the materials considered are listed in Table 1.

Table 1 Electromechanical Properties

| Material Properties | Aluminium | Gr/Ep | Foam | PIC 255 | PVDF |
|---|-----------|-------|-------|---------|--------|
| Mass Density | | | | | |
| ρ (kg/m ³) | 2769 | 1578 | 48 | 7800 | 1780 |
| Elastic Properties | | | | | |
| E_{11} (GPa) | 69 | 121.5 | 0.035 | 62.1 | 3.0 |
| E_{22} (GPa) | 69 | 10.4 | 0.035 | 62.1 | 3.0 |
| E_{33} (GPa) | 69 | 10.4 | 0.035 | 48.3 | 6.0 |
| G_{23} (GPa) | 28 | 5.1 | 0.014 | 21.7 | 1.0 |
| G_{13} (GPa) | 28 | 5.1 | 0.014 | 23.3 | 1.0 |
| G_{12} (GPa) | 28 | 5.1 | 0.014 | 23.3 | 1.0 |
| ν_{12} | 0.25 | 0.32 | 0.25 | 0.33 | 0.30 |
| ν_{13} | 0.25 | 0.32 | 0.25 | 0.43 | 0.30 |
| ν_{23} | 0.25 | 0.32 | 0.25 | 0.43 | 0.30 |
| Piezoelectric Properties | | | | | |
| d_{31} (10 ⁻¹² m/V) | - | - | - | -180 | -23 |
| d_{32} (10 ⁻¹² m/V) | - | - | - | -180 | -23 |
| d_{33} (10 ⁻¹² m/V) | - | - | - | 398 | 33 |
| Dielectric Properties | | | | | |
| ϵ_{33} (10 ⁻¹² Farad/m) | - | 27 | - | 10620 | 106000 |

5.1 [pvdf/0/foam]_s Sandwich Composite Plate with Piezoelectric Layers

The plate was square, having an edge length of 260 mm and a thickness aspect ratio of 21. It consisted of a 10 mm thick PVC foam core, Graphite/Epoxy composite faces each being 1 mm thick and two piezopolymer layers each being 0.2 mm thick. Simply-supported boundary conditions were assumed. The plate was hit at point P with coordinates ($L_x/3$, $L_y/8$) by a steel sphere, having a mass of 0.3 kg and an initial velocity of 1.8 m/s. A contact stiffness $k_y=6.65 \text{ e6 N/m}$, typical for a steel - Gr/Ep composite material contact [17], has been taken into account by assuming that the impactor will very soon locally compress the compliant piezopolymer and then contact will be dominated by the composite face. The plate was modeled using five discrete layers through-thickness, namely one for each material layer, and 9x9 bending vibration modes were considered.

Figure 4(a)-(b) illustrates the temporal variation of impact force and transverse displacement at the impact location. As expected, the through-thickness variable transverse displacement assumption in equation (1) yields a different deflection for top and bottom face. This trend can be also observed in Figure 4(c). A major advantage of the higher-order layerwise kinematics of the current methodology compared to linear layerwise ones is the prediction of interlaminar shear stress at the interface between adjacent discrete layers, as shown in Figure 4(d). This capability enables the construction of Figure 4(e)-(f), which show the time variation of out plane stresses at the interface between faces and core.

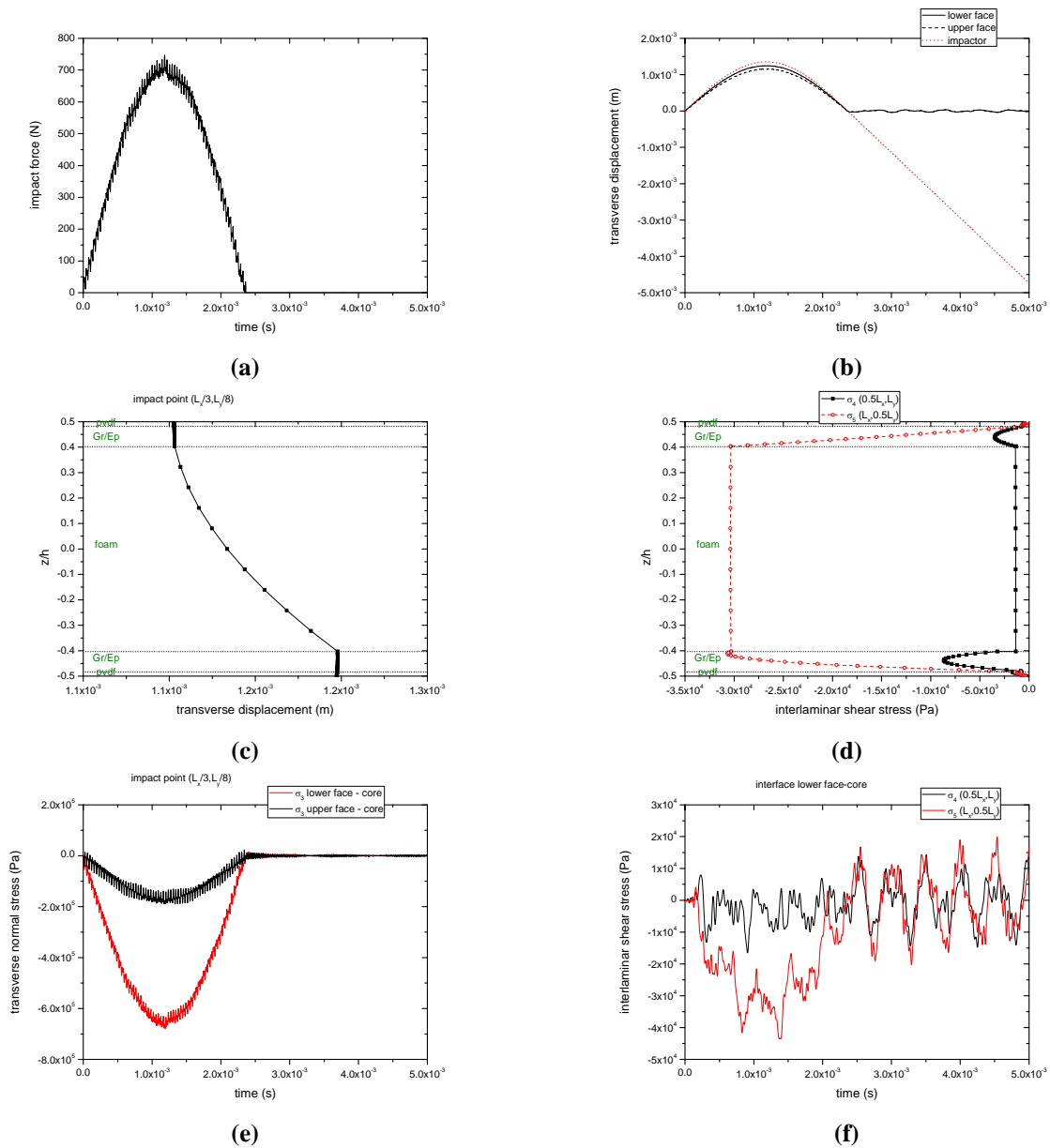


Figure 4: Global-local impact response of sandwich plate: (a) Impact force time history; (b) Temporal variation of transverse displacements at impact point; (c)-(d) Through-thickness variation of deflection and interlaminar shear stresses, respectively; (e)-(f) Out of plane stress time history at face-core interfaces.

5.2 Impact Identification in a Sandwich Composite Plate with Piezoelectric Patches

The sandwich plate was identical to the one studied above excluding the piezopolymer layers, which have been replaced by four PIC 255 piezoceramic patches (10x10x10 mm³). The patches were assumed to be placed at the quarters of the plate on the impacted face (Figure 5(a)). A steel impactor having a mass of 0.29 kg was assumed to hit the bottom face of the plate at (L_x/8, L_y/8) with an initial velocity of 1.8 m/s. The plate response has been predicted and the predictions were input for the impact identification technique described in section 3, which was implemented for backcalculating impact location, mass and velocity of impactor.

In Figure 5(b) the predicted sensory signals are shown. On the basis of these signals first estimations of the area around the impact location and the time t_d of disaggregation between impactor-plate (end of impact event) can be made. The low left quarter of the plate and the timestep at $t_d=2.5$ ms, when the signal of highest amplitude crosses zero, were chosen. A first scan through values of the four parameters to be identified (m_i , v_0 , x_p , y_p) is conducted within a preliminary range of ($[0.05$ kg, 0.5 kg], $[0.5$ m/s, 5 m/s], $[L_x/16, 7L_x/16]$, $[L_y/16, 7L_y/16]$), which resulted to a first estimate (0.3 kg, 2 m/s, $L_x/8$, $L_y/8$). The final estimated values have been obtained by assuming bounds at $\pm 20\%$ of the first estimates and using constrained optimization algorithms, as (0.293 kg, 1.83 m/s, 0.324 m, 0.322m). Figure 5(c)-(d) show predicted and backcalculated response for sensory signals and impact force history.

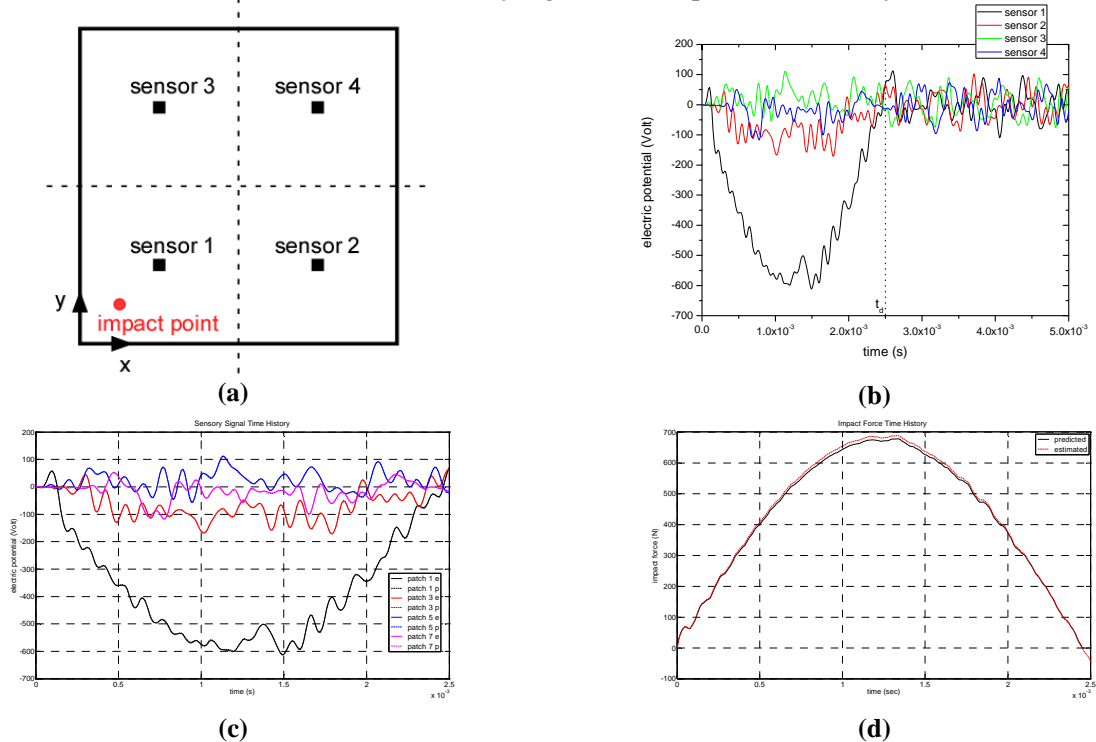


Figure 5: Impact identification in the case of a sandwich composite plate with piezoelectric patches: (a) Sensor location; (b) Sensory signals and estimated end of impact event t_d ; (c)-(d) Predicted and estimated sensory signals and impact force.

5.3 Impact Testing of Sandwich Plate with Piezoelectric Patches

The sandwich plate specimen consisted of 0.8 mm thick Aluminum faces and 10 mm thick PVC foam core. It was square and had an edge length of $a=0.26$ m. Four piezoceramic patches were attached on the surface opposite to the impacted face as shown in Figure 5(a). The impactor had an equivalent inertia of 0.293 kg and hit the plate at point $(7a/8, a/8)$ with an initial velocity measured as 0.28 m/s. Since no indentation measurements were available, a contact stiffness of $5e5$ N/m, being in a range typical for sandwich structures [22], has been used in the numerical model. The plate has been modeled using 3 discrete layers and 9×9 bending vibration modes.

Figure 6 show comparisons between predicted and measured values for impact force and sensory signals. Good correlation is observed between predicted and measured impact force and impact duration, whereas there is deviation in the case of the sensory signals. It is interesting that the maximum measured signal at the sensor closer to the impact location is around twice the predicted value, moreover, there was nearly no vibration measured after disaggregation. The deviations observed may be attributed to a lot of

parameters, which have not been taken into account in the numerical model, such as, effect of clamps at the plate boundaries, unequal piezoelectric coefficients in longitudinal and transverse in-plane direction, non-linear contact law, small tip for relative large inertia, which may cause local plasticity effects, and damping introduced by foam material and friction in the supports, which is neglected in the current formulation. The consideration of some of these parameters towards improvement of predictions will be a subject of work to follow.

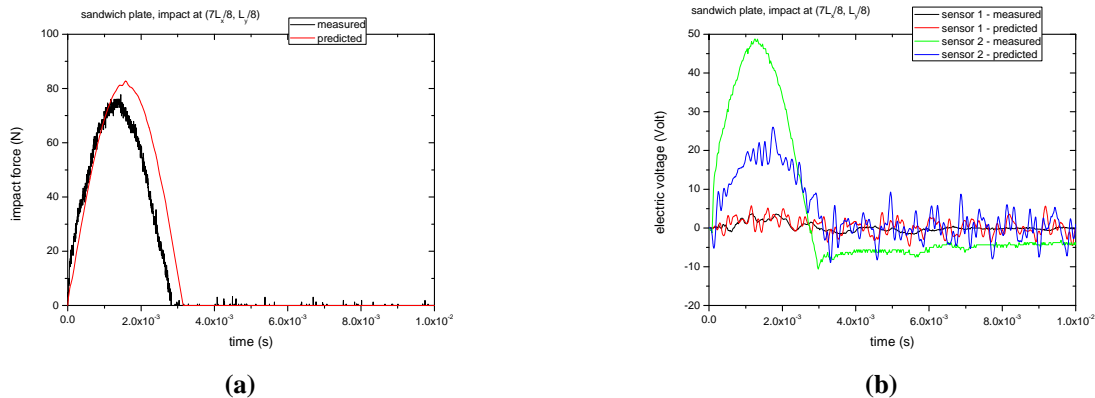


Figure 6: Comparison between predicted and measured values for a sandwich plate hit eccentrically: (a) Impact force; (b) Sensory signals.

6. SUMMARY

The presented higher-order layerwise impact mechanics methodology enables efficient prediction of both global and local through-thickness response of impacted sandwich plates with piezoelectric transducers. One of its major benefits lies in the prediction of stress at the interface between adjacent discrete layers. The methodology appears to be promising for posteriori impact identification of parameters such as impact location, impactor mass, velocity and material. Thus, the full impact event, including impact force time history and through-thickness stress distributions, may be reconstructed by using the acquired sensory signals. Validation studies with impact testing measurements have been conducted in a custom low-cost portable experimental configuration and revealed that the current numerical model accurately predicts impact force and duration in sandwich composite plates. The investigation of deviations observed between predicted and measured sensory signals will be a topic of future work.

ACKNOWLEDGMENTS

The research leading to the results presented in this work has received funding from the People Programme (Marie Curie Actions) of the European Unions' Seventh Framework Programme (FP7/2007-2013) under REA grant agreement n^o 299089.

REFERENCES

1. Abrate, S., "Localized Impact on Sandwich Structures with Laminated Facings," *Applied Mechanics Reviews*, Vol. 50, No. 2, 1997, pp. 69-82.
2. Chai, G. B., Zhu, S., "A Review of Low-Velocity Impact on Sandwich Structures," *Journal of Materials Design and Applications*, Vol. 225, 2011, pp. 207-230.

3. Olsson, R., "Closed Form Prediction of Peak Load and Delamination Onset under Small Mass Impact," *Composite Structures*, Vol. 59, No. 3, 2003, pp. 341-349.
4. Besant, T., Davies, G. A. O., Hitchings, D., "Finite Element Modelling of Low Velocity Impact of Composite Sandwich Panels," *Composites Part A*, Vol. 32, No. 9, 2001, pp. 1189-1196.
5. Christoforou, A. P., Yigit, A. S., Majeed, M., "Low-Velocity Impact Response of Structures with Local Plastic Deformation: Characterization and Scaling," *Journal of Computational and Nonlinear Dynamics*, Vol. 8, No. 1, 2013, pp. 011012-1-011012-10.
6. Olsson, R., McManus, H. L., "Improved Theory for Contact Indentation of Sandwich Panels," *AIAA Journal*, Vol. 34, No. 6, 1996, pp. 1238-1244.
7. Palazotto, A. N., Herup, E. J., Gummadi, L. N. B., "Finite Element Analysis of Low-Velocity Impact on Composite Sandwich Plates," *Composite Structures*, Vol. 49, No. 2, 2000, pp. 209-227.
8. Malekzadeh, K., Khalili, M. R., Olsson, R., Jafari, A., "Higher-order dynamic response of composite sandwich panels with flexible core under simultaneous low-velocity impacts of multiple small masses," *International Journal of Solids and Structures*, Vol. 43, No. 22-23, 2006, pp. 6667-6687.
9. Icardi, U., Ferrero, L., "Impact Analysis of Sandwich Composites Based on a Refined Plate Element with Strain Energy Updating," *Composite Structures*, Vol. 89, No. 1, 2009, pp. 35-51.
10. Choi, K., Chang F. K., "Identification of Foreign Object Impact in Structures using Distributed Sensors," *Journal of Intelligent Material Systems and Structures*, Vol. 5, No. 6, 1994, pp. 864-869.
11. Tracy, M., Chang, F. K., "Identifying Impacts in Composite Plates with Piezoelectric Strain Sensors, Part I: Theory," *Journal of Intelligent Material Systems and Structures*, Vol. 9, No. 11, 1998, pp. 920-928.
12. Park, J., Ha, S., Chang, F. K., "Monitoring Impact Events Using a System-Identification Method," *AIAA Journal*, Vol. 47, No. 9, 2009, pp. 2011-2021.
13. Abramovitch, H., Burgard, M., Ederly-Azulay, L., Evans, K. E., Hoffmesiter, M., Miller, W., Scarpa, F., Smith, C. W., Tee, K. F., "Smart Tetrachiral and Hexachiral Honeycomb: Sensing and Impact Detection," *Composites Science and Technology*, Vol. 70, No. 7, 2010, pp. 1072-1079.
14. Frieden, J., Cugnoni, J., Botsis, J., Gmür, T., 2012, "Low Energy Impact Damage Monitoring of Composites using Dynamic Strain Signals from FBG sensors: - Part II: Damage Identification", *Composite Structures*, Vol. 94, No. 2, 2012, pp. 593-600.
15. Liu, Y., Chattopadhyay, A., "Low-Velocity Impact Damage Monitoring of a Sandwich Composite Wing," *Journal of Intelligent Material Systems and Structures*, Vol. 24, No. 17, 2013, pp. 2074-2083.
16. Ghajari, M., Sharif-Khodaei, Z., Aliabadi, M. H., Apicella, A., "Identification of Impact Force for Smart Composite Stiffened Panels," *Smart Materials and Structures*, Vol. 22, 2013, 13 pp.
17. Saravanos, D. A., Christoforou, A. P., "Low-Energy Impact of Adaptive Cylindrical Piezoelectric-Composite Shells," *International Journal of Solids and Structures*, Vol. 39, No. 8, 2002, pp. 2257-2279.
18. Plagianakos, T. S., Papadopoulos, E. G., "Low-energy impact response of composite and sandwich composite plates with piezoelectric sensory layers," *International Journal of Solids and Structures*, Vol. 51, No. 14, 2014, pp. 2713-2727.
19. Plagianakos, T. S., Papadopoulos, E. G., "Higher-order 2-D/3-D layerwise mechanics and finite elements for composite and sandwich composite plates with piezoelectric layers," *submitted to Aerospace Science and Technology*.
20. Dugundji, J., "Simple Expressions for Higher Vibration Modes of Uniform Euler Beams," *AIAA Journal*, Vol. 26, No. 8, 1988, pp. 1013-1014.
21. Lika, K., "Design and Development of a 5-axis Force/Torque Sensor," MSc Thesis, 2013, Department of Mechanical Engineering, National Technical University of Athens, Greece.
22. Olsson, R., "Engineering method for prediction of impact response and damage in sandwich panels," *Journal of Sandwich Structures and Materials*, Vol. 4, No. 3, 2002, pp. 3-29.